Geophysical Research Letters

RESEARCH LETTER
10.1029/2020GL087876

Why Does the CP El Niño less Frequently Evolve Into La Niña than the EP El Niño?

Shan He[1,2], Jin-Yi Yu[2], Song Yang[1,3,4], and Shih-Wei Fang[2]

[1]School of Atmospheric Sciences, Sun Yat-sen University, Guangzhou, China, [2]Department of Earth System Science, University of California at Irvine, Irvine, CA, USA, [3]Guangdong Province Key Laboratory for Climate Change and Natural Disaster Studies, Sun Yat-sen University, Guangzhou, China, [4]Southern Marine Science and Engineering Guangdong Laboratory (Zhuhai), Guangdong, China

Key Points:
- The Central-Pacific (CP) El Niño decays and evolves into La Niña (38%) less frequently than the Eastern-Pacific (EP) El Niño (75%)
- The transitions involve a wind reversal in the western Pacific for the EP type and a wind shift in the central Pacific for the CP type
- The EP type aids its transitions via Indo-Pacific teleconnections, but the CP type impedes its transitions via subtropical teleconnections

Supporting Information:
- Supporting Information S1

Correspondence to:
S. Yang and J.-Y. Yu,
yangsong3@mail.sysu.edu.cn;
jyyu@uci.edu

Citation:
He, S., Yu, J.-Y., Yang, S., Fang, S.-W. (2020). Why does the CP El Niño less frequently evolve into La Niña than the EP El Niño?. *Geophysical Research Letters*, *47*, e2020GL087876. https://doi.org/10.1029/2020GL087876

Received 8 MAR 2020
Accepted 27 JUN 2020
Accepted article online 8 JUL 2020

Abstract During 1958–2017, the Central-Pacific (CP) El Niño evolved into La Niña less frequently (38%) than the Eastern-Pacific (EP) El Niño (75%). Composite analyses reveal that the reversal of zonal wind anomalies in the tropical western Pacific is the key mechanism for the EP El Niño's transitions to La Niña. This reversal induces oceanic Kelvin waves to promote the La Niña onset. This reversal mechanism is often triggered by the Indo-Pacific teleconnection produced by the EP El Niño. Consequently, the EP El Niño often experiences the transitional evolution. For the CP events, the southward shift of westerly anomalies in the tropical central Pacific is the key mechanism for transitions from El Niño to La Niña via local processes. However, the subtropical teleconnection of the CP El Niño prevents this mechanism from occurring and often causes the nontransitional evolution for the CP events.

Plain Language Summary Some El Niño events evolve into La Niña after their decay, but others do not. The La Niña events following an El Niño event often induce severe floods, causing deaths and substantial pecuniary loss. Knowing why an El Niño event can or cannot evolve into La Niña, we can predict the flood-causing La Niña. In this study, we examine the El Niño events during 1958–2017 and find that the Central-Pacific (CP) type of El Niño is less likely than the Eastern-Pacific (EP) type to evolve into La Niña after its decay. We conduct statistical analyses to uncover the causes of the difference. The difference mainly stems from the facts that these two types of El Niño have different transition mechanisms and that their teleconnections in the Indian Ocean and subtropical Pacific favor the transition mechanism for the EP type but impede the transition mechanism for the CP type.

1. Introduction

El Niño–Southern Oscillation (ENSO) is an ocean-atmosphere coupled phenomenon with profound climate impacts worldwide. However, the impacts are considerably different between its warm (i.e., El Niño) and cold (i.e., La Niña) phases, as well as among its different evolution patterns (e.g., Cai et al., 2010; Tokinaga et al., 2019). At least two primary evolution patterns exist. One is that an El Niño (a La Niña) event decays and then changes into a La Niña (an El Niño) event. The other is that an El Niño (a La Niña) event lingers for 2 years (McPhaden & Zhang, 2009; Yu & Fang, 2018). The lingering events have caused U.S. prolonged droughts (Cole et al., 2002), while the transitional events (e.g., La Niña following El Niño) have caused flash floods in Bangladesh and China (Terao et al., 2013; Wei et al., 2014).

Previous studies have identified several physical processes important to the event-to-event transitions of ENSO. Some processes reside within the tropical Pacific (e.g., F.-F. Jin, 1997; Ohba & Ueda, 2009; Okumura & Deser, 2010), and others originate in the extratropical Pacific (e.g., Y. Wang et al., 2013; Yu & Fang, 2018), tropical North Atlantic (e.g., Ham et al., 2013; L. Wang et al., 2017), or tropical Indian Ocean (e.g., Izumo et al., 2014). Within the tropical Pacific, ENSO-induced recharge/discharge of equatorial mean ocean heat content is a key mechanism to cause the transitions (Chen et al., 2016; F.-F. Jin, 1997; Wyrtki, 1975). Surface wind variations over the tropical western and central Pacific around the peak phase of ENSO have also been proven to be important to the transitions (e.g., Ohba & Ueda, 2009; Okumura & Deser, 2010; Weisberg & Wang, 1997). In the tropical western Pacific, a reversal of wind anomalies from westerlies to easterlies can excite upwelling Kelvin waves propagating to shoal the eastern Pacific thermocline, which changes El Niño to La Niña (Boulanger et al., 2003). In the tropical central Pacific, a southward shift

of El Niño's wind anomalies is part of the near-annual combination mode. It is caused by the seasonal migration of the belt of minimum wind speeds after autumn (McGregor et al., 2012; Stuecker et al., 2013). Due to surface westerly anomalies' southward shift, the climatological trade winds reoccur in the equatorial Pacific. Subsequently, the trade winds change El Niño into La Niña via increases in thermal damping, a thermocline slope, and upwelling (Vecchi & Harrison, 2006; Yu et al., 2010).

Between two flavors of ENSO, the equatorial thermocline variations play a key role in the Eastern-Pacific (EP) ENSO's evolutions, whereas the Central-Pacific (CP) ENSO' evolutions, alternatively known as the ENSO Modoki (Ashok et al., 2007), depends on zonal ocean advection, thermal damping, and extratropical Pacific forcing (Kug et al., 2009; Marathe et al., 2015; Yu et al., 2010; Yu & Kim, 2011). The event-to-event transition processes may differ between these two ENSO types and can cause different preferred evolution patterns. Kao and Yu (2009) noticed that the EP El Niño and La Niña tended to follow each other, forming an ENSO cycle, while the CP El Niño and La Niña tended to occur episodically. Ashok et al. (2017) also prove that the two types of El Niño show different evolutionary features of sea surface temperature (SST) and thermocline depth anomalies. The present study examines 21 El Niño events during 1958–2017, showing that the CP El Niño is less likely to evolve into La Niña than the EP El Niño (Figure S1, Table S1). Only 38% (five out of the 13 events) of the CP El Niño events are followed by La Niña events, in marked contrast to the EP El Niño events (75%; six out of the eight events). This difference indicates that the transition processes for these two types of El Niño might be different. In this study, we perform composite analyses to identify the key transition processes for each type of El Niño and to explain why the CP El Niño is less likely to be followed by La Niña than the EP El Niño.

2. Data and Methods

The following observational and reanalysis products were used in this study: (1) the monthly surface wind and sea level pressure (SLP) data from the National Centers for Environmental Prediction–National Center for Atmospheric Research (NCEP/NCAR) Reanalysis (Kalnay et al., 1996) and from the Japanese 55-year Reanalysis (JRA-55) (Kobayashi et al., 2015), (2) the monthly SST data from the Hadley Centre Sea Ice and SST (HadISST) data set (Rayner et al., 2003) and from the National Oceanic and Atmospheric Administration Extended Reconstructed SST (NOAA ERSST) version 5 data set (Huang et al., 2017), and (3) the monthly sea surface height (SSH) from the Simple Ocean Data Assimilation ocean/sea ice reanalysis (SODA) Version 2.2.4 (Carton & Giese, 2008) and from the German contribution to the Estimating the Circulation and Climate of the Ocean project (GECCO) ocean synthesis version 3 (Köhl, 2020). The NCEP/NCAR Reanalysis I, HadISST, and SODA V2.2.4 are used to produce results unless otherwise specified. Monthly anomalies are employed to remove the annual climatology. The monthly climatology is calculated based on the 1958–2017 period, except the climatology of SODA 2.2.4 (based on the 1958–2010 period) and the JRA-55 (based on the 1958–2012 period). Linear trends are removed from the anomalies.

In this study, the El Niño events chosen are the same as those identified by NCEP's Climate Prediction Center based on the Oceanic Niño index. The types of these El Niño events are determined by the consensus method of Yu et al. (2012) (Table S2), which draws upon the consensus of the identifications made by a EP/CP index method (Kao & Yu, 2009), a El Niño Modoki index method (Ashok et al., 2007), and a NIÑO3/4 index method (Yeh et al., 2009). We also use the EP and CP indices of Kao and Yu (2009). To calculate the EP index, we apply an empirical orthogonal function (EOF) analysis to the tropical Pacific SST anomalies after removing the NIÑO4-index-regressed parts of the anomalies. The time series of the leading EOF mode is used as the EP index. We use a similar method to calculate the CP index, except that the EOF analysis is applied to the SST anomalies after removing the NIÑO1 + 2-index-regressed parts of the anomalies. In order to identify the transition processes that change an El Niño phase of a certain year to a La Niña phase in the following year, the following classification is used to identify transitional and nontransitional events. A transitional El Niño event is defined as the El Niño event that decays and changes to a La Niña event during the following year. In addition, a nontransitional event is defined as the El Niño event that decays but remains in an El Niño state or a neutral state during the following year (Table S1). A 2-year El Niño event (e.g., the 1986/1988 or 2014/2016 events) is considered as two 1-year events, so their transition processes can be studied separately. We define the tropical western Pacific as between 10°S–10°N and 120°–160°E, and the tropical central Pacific as between 10°S–10°N and 160°E–120°W.

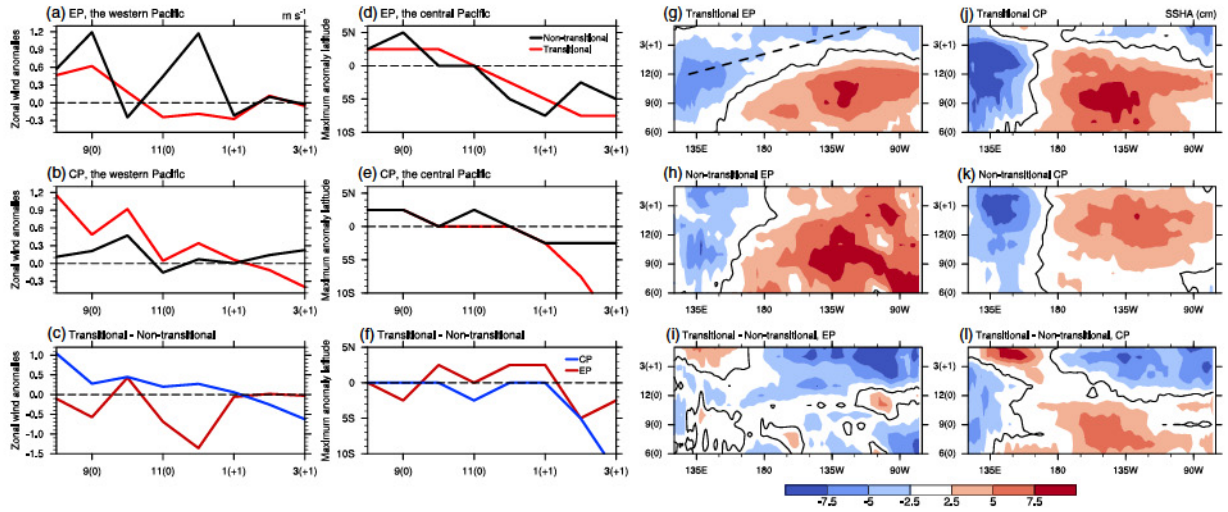

Figure 1. Temporal evolutions of both (a, b, c) the composite surface zonal wind anomalies over the tropical western Pacific (10°S–10°N and 120°–160°E) and (d, e, f) the latitude of the maximum westerly of the zonal mean composite anomalies in the tropical central Pacific (10°S–10°N and 160°E–120°W). The evolution diagrams present not only the transitional and nontransitional groups of the EP (upper panels) and CP (middle panels) El Niño events but also the transitional group minus the nontransitional group (lower panels). The Hovmöller diagrams displaying the composite SSH anomalies averaged between 5°S–5°N for the transitional (upper panels), nontransitional (middle panels), and transitional minus nontransitional (lower panels) groups of the (g, h, i) EP and (j, k, l) CP El Niño. The composite values are calculated after the anomalies of each El Niño event were scaled. The temporal evolutions displayed are from the developing August to decaying March in the six leftmost panels and from the developing June to decaying May in the six rightmost panels. Black lines in the six rightmost panels denote zero contours. (g) The dashed line indicates the propagation path of the upwelling Kelvin wave.

We apply a centered finite difference operation to calculate SSH anomaly tendencies. The term "scaled" is used during the composite analyses to describe the variables divided by DJF Niño 3.4 index. The scaled variables are used to diminish the influence of strong El Niño events and to weigh equal attention to all events. After a Fisher transformation, a 95% confidence level is applied to test whether the true partial correlation coefficient is equal to zero.

3. Transition Mechanisms for the Two Types of El Niño

To identify the transition mechanisms, we first examine the discharge process by contrasting the variations of the mean SSH averaged along the equatorial Pacific between the EP and CP El Niño (Figure S2). Consistent with previous studies (e.g., Ren & Jin, 2013), we find that the discharge is stronger in the EP El Niño than in the CP El Niño (Figure S2a). However, since the CP El Niño is typically weaker than the EP El Niño, the amount of ocean heat content that needs discharge to change the El Niño to La Niña is less for the CP type than for the EP type. Therefore, the weaker discharge cannot fully explain why the CP El Niño evolves to La Niña less frequently. In particular, we find that the difference in the discharge is smaller between the transitional and nontransitional groups of the CP El Niño than the EP El Niño (Figures S2b and S2c). Other processes exist to control the El Niño transitions, particularly the CP El Niño.

We then examine the evolutions of the surface zonal wind anomalies in the tropical western and central Pacific. In the tropical western Pacific during the EP El Niño, the wind anomalies of the transitional group change from westerlies to easterlies around November, but the anomalies of the nontransitional group are mostly westerlies from the developing August to the decaying March (Figures 1a, 1c, S3a, and S3b). During the CP El Niño, both the transitional and nontransitional groups are characterized by westerly anomalies throughout most of the developing and decaying stages (Figures 1b, 1c, S3c, and S3d). In the tropical central Pacific during the CP El Niño, the maximum westerly anomalies in the transitional group shift southward from around 3°N in the developing autumn to 8°S in the peak winter, and easterly anomalies prevail since the decaying March (Figures 1e and S3g). However, the nontransitional group's maximum anomalies remain near the equator throughout the developing to decaying stages (Figures 1e and S3h). During the EP El Niño, both the transitional and nontransitional groups feature a similar southward shift of the maximum westerly anomalies (Figures 1d, 1f, S3e, and S3f). These results indicate that the southward shift of

westerly anomalies in the central Pacific is a key feature for the transitions from the CP El Niño to La Niña, but this feature is unimportant for the EP El Niño's transitions. The key feature for the EP El Niño's transitions is the reversal of the zonal wind anomalies in the western Pacific. Note that despite a late wind reversal (after the decaying February) during the transitional CP events (Figure 1b), this is unimportant for the transition given the deep thermocline in spring (Y. Jin et al., 2019) (Text S1).

We next examine the evolutions of SSH anomalies to understand why the wind reversal causes the EP El Niño's transition and why the southward wind shift causes the CP El Niño's transition. During both types of El Niño, SSH anomalies in the equatorial central-eastern Pacific change from positive to negative after the peak phase of the transitional groups (Figures 1g and 1j) but maintain positive in the nontransitional groups (Figures 1h and 1k). The sign change is the key difference between the transitional and nontransitional groups of both El Niño types (Figures 1i and 1l). A decrease in the SSH anomalies (i.e., thermocline shoaling) cools down local SSTs, causing a La Niña condition. The sign change develops more in situ in the transitional CP El Niño composite (Figures 1j and 1l) but is more associated with the negative SSH anomalies propagating from the western Pacific in the transitional EP El Niño composite (Figures 1g and 1i). The negative anomalies start to propagate in the developing autumn when the wind reversal occurs in the western Pacific (cf. Figures 1a and 1c). The eastward propagation of the negative SSH anomalies during the transitional EP El Niño indicates that the reversal to easterly anomalies triggers upwelling Kelvin waves that propagate into the eastern Pacific, changing the EP El Niño to La Niña during the following months. During the transitional CP El Niño, the negative SSH anomalies emerge in the tropical central Pacific (Figures 1j and 1l) where the southward wind shift occurs (cf. Figures 1e and 1f). Due to this southward shift, climatological surface easterlies prevail in the tropical central Pacific. As part of the combination mode, the prevailing easterlies and southward-displaced westerly anomalies can transport positive SSH anomalies (i.e., ocean heat content) from the equator to around 10°N through Ekman transport (McGregor et al., 2012; Stuecker et al., 2013). This transport is strong in both the transitional and nontransitional EP events (Figures S4a–S4j) but weak in the transitional CP events (Figures S4k–S4o). This implies a minor role of the Ekman transport suggested by the combination mode in the EP El Niño's transition. The in situ decrease in the equatorial heat content (Figures S4k–S4o) implies an anomalous heat transport from ocean to the atmosphere. Specifically, the southward wind shift increases equatorial surface wind speeds and thus changes the CP El Niño to La Niña through latent heat flux anomalies (Li et al., 2018). Note that the positive equatorial SSH anomalies can be reflected at the eastern boundary, becoming off-equatorial anomalies. These off-equatorial anomalies can later terminate the El Niño through zonal oceanic transports (Chen et al., 2016).

Overall, these results indicate the transition of the EP El Niño is controlled more by remote wind variations in the tropical western Pacific through thermocline variations, while the CP El Niño's transition occurs due to local wind variations and the surface ocean heat fluxes over the tropical central Pacific. These findings support previous studies that thermocline dynamics control the EP ENSO while mixed-layer thermodynamics control the CP ENSO (Kao & Yu, 2009; Kug et al., 2009; Yu & Fang, 2018). These findings also explain why the southward wind shift in the tropical central Pacific is less effective than the wind reversal in the tropical western Pacific in distinguishing the transitional EP El Niño from the nontransitional EP El Niño. The southward shift of El Niño's wind anomalies in the tropical central Pacific is caused by the seasonal migration of the minimum wind speed belt after autumn (McGregor et al., 2012; Stuecker et al., 2013). Therefore, the shift should occur during all El Niño events. Interestingly, this shift is absent from the nontransitional CP El Niño, and the reasons are discussed in section 4.

To verify the above results, we repeat our analyses using the JRA-55 and GECCO3 data sets. We also conduct case studies with the 1972/1973 transitional EP event, 1986/1987 nontransitional EP event, 1987/1988 transitional CP event, and 1991/1992 nontransitional CP event. The results yielded from the JRA-55 and GECCO3 (Figures S5 and S6) and the case studies (Text S2, Figures S7 and S8) are consistent with the composite analysis results of the NCEP/NCAR Reanalysis and SODA 2.2.4 (cf. Figures 1 and S3).

4. Dependence of the Wind Patterns During Transitions on the Two Types of El Niño

Based on the transition mechanisms identified above, we explore the reasons for the CP El Niño's less frequent transition into La Niña. One possibility is that the EP El Niño can frequently induce its

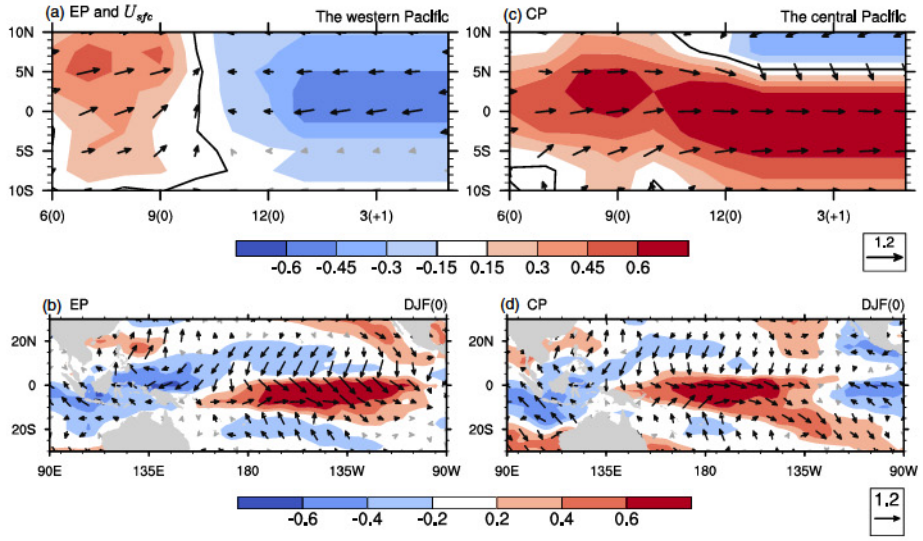

Figure 2. (a, c) The Hovmöller diagrams displaying the meridional profiles of the lead-lagged partial correlations between the DJF values of the EP (CP) index defined by Kao and Yu (2009) and the zonal mean of surface wind anomalies (vectors) conditional on the DJF CP (EP) index in the (a) tropical western Pacific and (c) tropical central Pacific from June to the following May. (b, d) The DJF spatial structures of the partial correlations with the (b) EP El Niño and (d) CP El Niño. The vectors in black denote the regions where the true partial correlation coefficient is not equal to zero at the 95% confidence level. Colors denote the zonal components of the correlations. Black lines in the upper panels denote the zero contours of the zonal components.

corresponding transition wind pattern (i.e., the wind reversal), but the CP El Niño can frequently impede its corresponding transition wind pattern (i.e., the southward wind shift). This possibility is examined by calculating the lead-lagged partial correlations between the EP index and the anomalies of surface zonal winds in the tropical western Pacific conditional on the CP index (Figures 2a and 2b) and between the CP index and the wind anomalies in the tropical central Pacific conditional on the EP index (Figures 2c and 2d). The calculations only use the DJF (i.e., the typical peak season of El Niño) values of the EP and CP indices, while the wind anomalies span from the developing June to the decaying May. Meanwhile, the calculations exclude La Niña months (Table S3). Figure 2a shows that the partial correlations with the EP index change from significantly positive values to significantly negative values around the developing November. In this period, wind reversal is observed in the tropical western Pacific during the transitional EP El Niño (Figures 1a and S3a). Figure 2b shows that anomalous surface easterlies (i.e., negative correlations) significantly appear over the tropical western Pacific during the DJF season of the EP El Niño. These results indicate that the EP El Niño can itself induce the wind reversal critical to its transition to La Niña.

In contrast, the southward shift of the westerly anomalies in the tropical central Pacific is absent from the partial correlations with the CP index (Figures 2c and 2d). The correlations remain significantly positive in the tropical central Pacific throughout the CP El Niño event. Additionally, the maximum correlations are confined to the equator, only shifting slightly from 3°N to 1°S around the developing November (Figures 2c and 2d). The range of this shift is much smaller than that observed during the transitional CP El Niño (cf. Figures 1e and S3g). These results suggest that the CP El Niño cannot itself induce a southward shift of the westerly anomalies necessary for its transitions to La Niña. These correlation features do not depend on the EP and CP indices chosen. Similar results appear when we use the indices defined by Yeh et al. (2009) (Figure S9).

Despite the dependence of the reversal in western Pacific winds on the EP El Niño, there still exist two non-transitional EP El Niño events. To explore the possible causes, we compare the composite anomalies of SLP and SST during the nontransitional EP El Niño in the peak DJF season with the composite anomalies during the transitional EP El Niño (Figures 3a–3f). There are two obvious differences in these figures: Firstly, the anomalous surface western North Pacific anticyclone induced by El Niño (B. Wang et al., 2000) is weaker

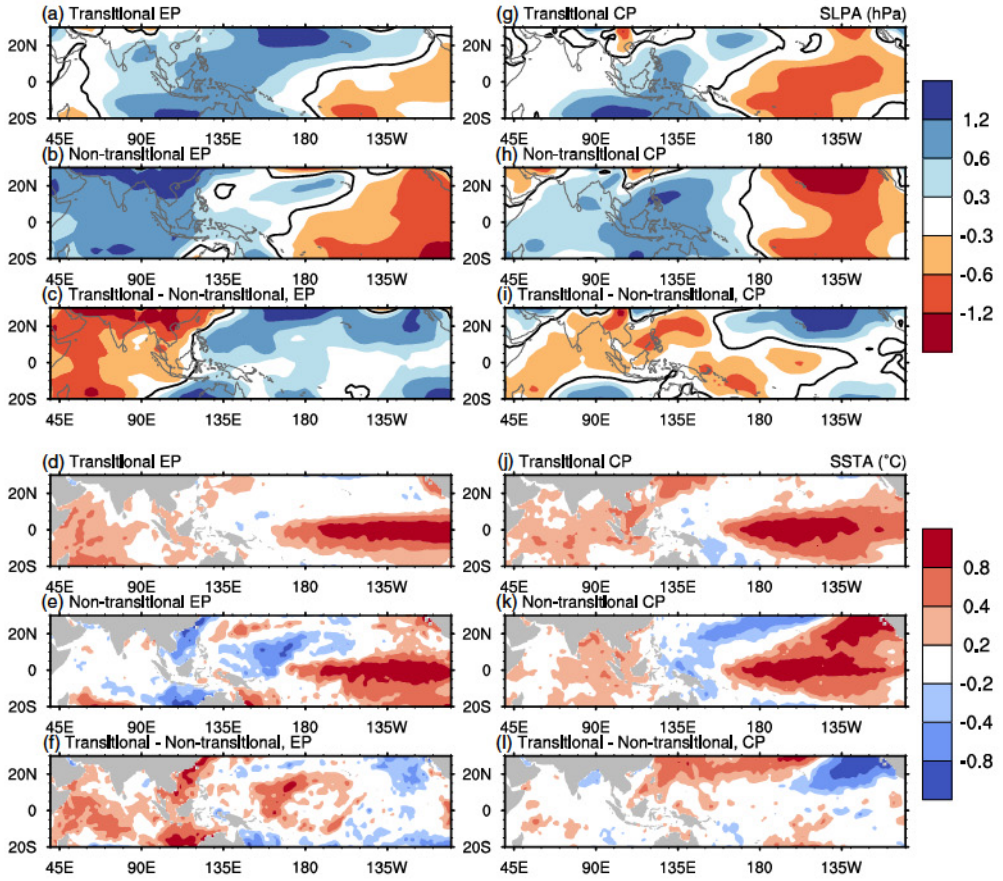

Figure 3. Composite values of the scaled SLP (upper six panels) and SST (lower six panels) anomalies during the peak DJF season for the (a, d, g, j) transitional, (b, e, h, k) nontransitional, and (c, f, i, l) transitional minus nontransitional groups of the EP (left panels) and CP (right panels) El Niño. Black lines denote zero contours (upper six panels).

in the nontransitional events (Figures 3a–3c). Secondly, the Indian Ocean basin warming induced by El Niño (Klein et al., 1999) is absent from the nontransitional events, while the warming occurs during the transitional events (Figures 3d–3f). Both the anomalous anticyclone and Indian Ocean warming can induce surface easterly anomalies in the western Pacific (Wu et al., 2010), causing a wind reversal. Since the conventional EP El Niño can lead to these two phenomena (Klein et al., 1999; B. Wang et al., 2000), most EP El Niño events are transitional events. The nontransitional events occur probably when other factors (e.g., the Australian monsoon variations and the Madden-Julian oscillation) interfere with the anomalous anticyclone and Indian Ocean warming induced by the EP El Niño (Benthuysen et al., 2018; Jia et al., 2011).

We also compare the composite anomalies of SLP and SST during the transitional CP El Niño with those during the nontransitional CP El Niño (Figures 3g–3l). The transitional group also features an Indian Ocean basin warming and an anomalous anticyclone in the northwestern Pacific during the peak DJF season (Figures 3g and 3j). As mentioned above, these two features should have produced surface easterly anomalies in the tropical western Pacific. However, we do not observe a reversal of western Pacific winds during the peak DJF season of the transitional CP El Niño (Figures 1b and S3c). A possible explanation is that the SST anomalies of the CP El Niño (Figure 3j) are located west of those in the EP El Niño (cf. Figure 3d). Therefore, the westerly anomalies of the CP El Niño are displaced westward in winter to cover the tropical western Pacific, canceling out the easterly anomalies produced by the Indian Ocean warming and the subtropical anticyclone (Yuan & Yang, 2012). A similar mutual cancellation also occurs in the nontransitional group between the displaced westerly anomalies and the easterly anomalies produced by the anomalous anticyclone over the northwestern Pacific (Figures 3h and 3k). Therefore, there is no reversal in the western Pacific winds in either CP El Niño group.

The key difference between these two CP El Niño groups is that the nontransitional group features a band of positive SST anomalies extending from Baja California toward the tropical central Pacific (Figures 3k and 3l). These SST anomalies are accompanied by an anomalous cyclone over the subtropical eastern Pacific (Figures 3h and 3i). The anomalous cyclone maintains the surface westerly anomalies in the tropical central Pacific, preventing the southward shift of the central Pacific winds in the nontransitional group (Figures 1e and S3h). These features resemble those of the Pacific meridional mode (Chiang & Vimont, 2004) that used to be considered as a major feature of the CP El Niño (Stuecker, 2018; Yu et al., 2010). Therefore, the subtropical anomalies accompanying the CP El Niño prevent the southward wind shift and impede the transitions to La Niña. Recent studies point out that a few CP El Niño events do not exhibit this feature (C. Wang & Wang, 2013). All these results together suggest that the features of the Pacific meridional mode that frequently accompanies the CP El Niño events can prevent the southward shift of the central Pacific winds and impede the transitions to La Niña. Therefore, the CP El Niño is often nontransitional.

To verify the results from the composite analysis in this section, we repeat our analyses using the JRA-55 and NOAA ERSST V5 data sets. Additionally, we again conduct case studies with the 1972/1973, 1986/1987, 1987/1988, and 1991/1992 El Niño events. The results yielded from the JRA-55 and NOAA ERSST V5 (Figure S10) and the case studies (Text S3, Figure S11) support the composite analysis results of the NCEP/NCAR Reanalysis and HadISST (cf. Figure 3).

5. Conclusions

This study explores why most of the CP El Niño events do not evolve to La Niña, but most of the EP El Niño events do. Our results reveal that these two types of El Niño self-induce their preferred evolution patterns. The EP El Niño's typical teleconnection induces anomalous Indian Ocean warming and western North Pacific anticyclone, which can activate the wind reversal mechanism in the western Pacific to change the EP El Niño to La Niña. On the other hand, the subtropical Pacific anomalies typically accompanying the CP El Niño can prevent the southward wind shift mechanism over the tropical central Pacific to impede the transition of the CP El Niño to La Niña. These findings explain how and why El Niño exhibits a variety of event-to-event transitions. However, while we have conducted case studies to verify the results obtained from the composite analyses, the findings are obtained with a small number of the EP/CP El Niño events available in observations. The small sample size increases the likelihood of a Type II error. On the other hand, although reanalysis products are capable of reproducing the interannual variability, there exist uncertainties among them (e.g., Long et al., 2017; Marathe et al., 2015). Long-term simulations with climate models or advanced statistical techniques will help to further verify the findings. Furthermore, the occurrences of the EP/CP El Niño can be altered by slow changes in the Pacific mean state (e.g., Jadhav et al., 2015). However, its influences on the transitions of the EP/CP El Niño have remained unclear, and further studies are needed.

Data Availability Statement

The NCAR Command Language software (Version 6.5.0) is obtained at https://doi.org/10.5065/D6WD3XH5, the NCEP/NCAR Reanalysis I and NOAA ERSST V5 at https://www.esrl.noaa.gov/psd/, the JRA-55 at https://jra.kishou.go.jp/, HadISST at https://www.metoffice.gov.uk, SODA2 at https://www.atmos.umd.edu/~ocean/, GECCO3 at https://icdc.cen.uni-hamburg.de/en/icdc.html, and the years of El Niño (https://origin.cpc.ncep.noaa.gov/).

Acknowledgments

We thank three anonymous reviewers for their constructive and helpful comments. We acknowledge the support from the National Key R&D Program of China under grant 2019YFC1510400, the National Natural Science Foundation of China under grants 41690123 and 41690120, the NSF's Climate & Large-scale Dynamics Program of the United States under grant AGS1833075, and the China Postdoctoral Science Foundation funded project (2019M663205). To all these organizations or platforms, we extend our sincere thanks. Our gratitude also goes to Ms. Ge Tang for her kind help in polishing this paper.

References

Ashok, K., Behera, S. K., Rao, S. A., Weng, H., & Yamagata, T. (2007). El Niño Modoki and its possible teleconnection. *Journal of Geophysical Research*, *112*, C11007. https://doi.org/10.1029/2006JC003798

Ashok, K., Shamal, M., Sahai, A. K., & Swapna, P. (2017). Nonlinearities in the evolutional distinctions between El Niño and La Niña types. *Journal of Geophysical Research: Oceans*, *122*, 9649–9662. https://doi.org/10.1002/2017JC013129

Benthuysen, J. A., Oliver, E. C. J., Feng, M., & Marshall, A. G. (2018). Extreme marine warming across tropical Australia during austral summer 2015–2016. *Journal of Geophysical Research: Oceans*, *123*, 1301–1326. https://doi.org/10.1002/2017JC013326

Boulanger, J.-P., Cravatte, S., & Menkes, C. (2003). Reflected and locally wind-forced interannual equatorial Kelvin waves in the western Pacific Ocean. *Journal of Geophysical Research*, *108*(C10), 3311. https://doi.org/10.1029/2002JC001760

Cai, W., van Rensch, P., Cowan, T., & Sullivan, A. (2010). Asymmetry in ENSO teleconnection with regional rainfall, its multidecadal variability, and impact. *Journal of Climate*, *23*(18), 4944–4955. https://doi.org/10.1175/2010JCLI3501.1

Carton, J. A., & Giese, B. S. (2008). A reanalysis of ocean climate using Simple Ocean Data Assimilation (SODA). *Monthly Weather Review*, *136*(8), 2999–3017. https://doi.org/10.1175/2007MWR1978.1

Chen, H.-C., Hu, Z.-Z., Huang, B., & Sui, C.-H. (2016). The role of reversed equatorial zonal transport in terminating an ENSO event. *Journal of Climate*, *29*, 5859–5877. https://doi.org/10.1175/JCLI-D-16-0047.1

Chiang, J. C. H., & Vimont, D. J. (2004). Analogous Pacific and Atlantic meridional modes of tropical atmosphere-ocean variability. *Journal of Climate*, *17*(21), 4143–4158. https://doi.org/10.1175/JCLI4953.1

Cole, J. E., Overpeck, J. T., & Cook, E. R. (2002). Multiyear La Niña events and persistent drought in the contiguous United States. *Geophysical Research Letters*, *29*(13). https://doi.org/10.1029/2001GL013561

Ham, Y.-G., Kug, J.-S., Park, J.-Y., & Jin, F.-F. (2013). Sea surface temperature in the north tropical Atlantic as a trigger for El Niño/Southern Oscillation events. *Nature Geoscience*, *6*, 112–116. https://doi.org/10.1038/ngeo1686

Huang, B., Thorne, P. W., Banzon, V. F., Boyer, T., Chepurin, G., Lawrimore, J. H., et al. (2017). Extended reconstructed sea surface temperature, version 5 (ERSSTv5): Upgrades, validations, and intercomparisons. *Journal of Climate*, *30*(20), 8179–8205. https://doi.org/10.1175/JCLI-D-16-0836.1

Izumo, T., Lengaigne, M., Vialard, J., Luo, J.-J., Yamagata, T., & Madec, G. (2014). Influence of Indian Ocean dipole and Pacific recharge on following year's El Niño: Interdecadal robustness. *Climate Dynamics*, *42*, 291–310. https://doi.org/10.1007/s00382-012-1628-1

Jadhav, J., Panickal, S., Marathe, S., & Ashok, K. (2015). On the possible cause of distinct El Ninō types in the recent decades. *Scientific Reports*, *5*(1), 17,009. https://doi.org/10.1038/srep17009

Jia, X., Chen, L., Ren, F., & Li, C. (2011). Impacts of the MJO on winter rainfall and circulation in China. *Advances in Atmospheric Sciences*, *28*(3), 521–533. https://doi.org/10.1007/s00376-010-9118-z

Jin, F.-F. (1997). An equatorial ocean recharge paradigm for ENSO. Part I: Conceptual model. *Journal of the Atmospheric Sciences*, *54*(7), 811–829. https://doi.org/10.1175/1520-0469(1997)054<0811:AEORPF>2.0.CO;2

Jin, Y., Liu, Z., Lu, Z., & He, C. (2019). Seasonal cycle of background in the tropical Pacific as a cause of ENSO spring persistence barrier. *Geophysical Research Letters*, *46*, 13371–13378. https://doi.org/10.1029/2019GL085205

Kalnay, E., Kanamitsu, M., Kistler, R., Collins, W., Deaven, D., Gandin, L., et al. (1996). The NCEP/NCAR 40-year reanalysis project. *Bulletin of the American Meteorological Society*, *77*(3), 437–471. https://doi.org/10.1175/1520-0477(1996)077<0437:TNYRP>2.0.CO;2

Kao, H.-Y., & Yu, J.-Y. (2009). Contrasting Eastern-Pacific and Central-Pacific types of ENSO. *Journal of Climate*, *22*(3), 615–632. https://doi.org/10.1175/2008JCLI2309.1

Klein, S. A., Soden, B. J., & Lau, N.-C. (1999). Remote sea surface temperature variations during ENSO: Evidence for a tropical atmospheric bridge. *Journal of Climate*, *12*(4), 917–932. https://doi.org/10.1175/1520-0442(1999)012<0917:RSSTVD>2.0.CO;2

Kobayashi, S., Ota, Y., Harada, Y., Ebita, A., Moriya, M., Onoda, H., et al. (2015). The JRA-55 reanalysis: General specifications and basic characteristics. *Journal of the Meteorological Society of Japan*, *93*(1), 5–48. https://doi.org/10.2151/jmsj.2015-001

Köhl, A. (2020). Evaluating the GECCO3 1948–2018 ocean synthesis—A configuration for initializing the MPI-ESM climate model. *Quarterly Journal of the Royal Meteorological Society*, qj.3790. https://doi.org/10.1002/qj.3790

Kug, J.-S., Jin, F.-F., & An, S.-I. (2009). Two types of El Niño events: Cold tongue El Niño and warm pool El Niño. *Journal of Climate*, *22*(6), 1499–1515. https://doi.org/10.1175/2008JCLI2624.1

Li, H., Xu, H., Li, Z., & Deng, J. (2018). Different evolution features for two types of El Niño and possible causes for these differences. *International Journal of Climatology*, *38*(7), 2967–2979. https://doi.org/10.1002/joc.5476

Long, C. S., Fujiwara, M., Davis, S., Mitchell, D. M., & Wright, C. J. (2017). Climatology and interannual variability of dynamic variables in multiple reanalyses evaluated by the SPARC Reanalysis Intercomparison Project (S-RIP). *Atmospheric Chemistry and Physics*, *17*(23), 14,593–14,629. https://doi.org/10.5194/acp-17-14593-2017

Marathe, S., Ashok, K., Swapna, P., & Sabin, T. P. (2015). Revisiting El Niño Modokis. *Climate Dynamics*, *45*(11–12), 3527–3545. https://doi.org/10.1007/s00382-015-2555-8

McGregor, S., Timmermann, A., Schneider, N., Stuecker, M. F., & England, M. H. (2012). The effect of the South Pacific convergence zone on the termination of El Niño events and the meridional asymmetry of ENSO. *Journal of Climate*, *25*(16), 5566–5586. https://doi.org/10.1175/JCLI-D-11-00332.1

McPhaden, M. J., & Zhang, X. (2009). Asymmetry in zonal phase propagation of ENSO sea surface temperature anomalies. *Geophysical Research Letters*, *36*, L13703. https://doi.org/10.1029/2009GL038774

Ohba, M., & Ueda, H. (2009). Role of nonlinear atmospheric response to SST on the asymmetric transition process of ENSO. *Journal of Climate*, *22*(1), 177–192. https://doi.org/10.1175/2008JCLI2334.1

Okumura, Y. M., & Deser, C. (2010). Asymmetry in the duration of El Niño and La Niña. *Journal of Climate*, *23*(21), 5826–5843. https://doi.org/10.1175/2010JCLI3592.1

Rayner, N. A., Parker, D. E., Horton, E. B., Folland, C. K., Alexander, L. V., Rowell, D. P., et al. (2003). Global analyses of sea surface temperature, sea ice, and night marine air temperature since the late nineteenth century. *Journal of Geophysical Research*, *108*(D14), 4407. https://doi.org/10.1029/2002JD002670

Ren, H.-L., & Jin, F.-F. (2013). Recharge oscillator mechanisms in two types of ENSO. *Journal of Climate*, *26*(17), 6506–6523. https://doi.org/10.1175/JCLI-D-12-00601.1

Stuecker, M. F. (2018). Revisiting the Pacific meridional mode. *Scientific Reports*, *8*(1), 3216. https://doi.org/10.1038/s41598-018-21537-0

Stuecker, M. F., Timmermann, A., Jin, F.-F., McGregor, S., & Ren, H.-L. (2013). A combination mode of the annual cycle and the El Niño/Southern Oscillation. *Nature Geoscience*, *6*(7), 540–544. https://doi.org/10.1038/ngeo1826

Terao, T., Murata, F., Habib, A., Bhuiyan, S. H., Choudhury, S. A., & Hayashi, T. (2013). Impacts of rapid warm-to-cold ENSO transitions on summer monsoon rainfall over the northeastern Indian subcontinent. *Journal of the Meteorological Society of Japan*, *91*(1), 1–21. https://doi.org/10.2151/jmsj.2013-101

Tokinaga, H., Richter, I., & Kosaka, Y. (2019). ENSO influence on the Atlantic Niño, revisited: Multi-year versus single-year ENSO events. *Journal of Climate*, *32*(14), 4585–4600. https://doi.org/10.1175/JCLI-D-18-0683.1

Vecchi, G. A., & Harrison, D. E. (2006). The termination of the 1997–98 El Niño. Part I: Mechanisms of oceanic change. *Journal of Climate*, *19*(12), 2633–2646. https://doi.org/10.1175/JCLI3776.1

Wang, B., Wu, R., & Fu, X. (2000). Pacific–east Asian teleconnection: How does ENSO affect east Asian climate? *Journal of Climate*, *13*(9), 1517–1536. https://doi.org/10.1175/1520-0442(2000)013<1517:PEATHD>2.0.CO;2

Wang, C., & Wang, X. (2013). Classifying El Niño Modoki I and II by different impacts on rainfall in southern China and typhoon tracks. *Journal of Climate*, *26*(4), 1322–1338. https://doi.org/10.1175/JCLI-D-12-00107.1

Wang, L., Yu, J.-Y., & Paek, H. (2017). Enhanced biennial variability in the Pacific due to Atlantic capacitor effect. *Nature Communications*, *8*(1), 14,887. https://doi.org/10.1038/ncomms14887

Wang, Y., Lupo, A. R., & Qin, J. (2013). A response in the ENSO cycle to an extratropical forcing mechanism during the El Niño to La Niña transition. *Tellus Series A: Dynamic Meteorology and Oceanography*, *65*(1), 22,431. https://doi.org/10.3402/tellusa.v65i0.22431

Wei, W., Chang, Y., & Dai, Z. (2014). Streamflow changes of the Changjiang (Yangtze) River in the recent 60 years: Impacts of the East Asian summer monsoon, ENSO, and human activities. *Quaternary International*, *336*, 98–107. https://doi.org/10.1016/j.quaint.2013.10.064

Weisberg, R. H., & Wang, C. (1997). A western Pacific oscillator paradigm for the El Niño–Southern Oscillation. *Geophysical Research Letters*, *24*(7), 779–782. https://doi.org/10.1029/97GL00689

Wu, B., Li, T., & Zhou, T. (2010). Relative contributions of the Indian Ocean and local SST anomalies to the maintenance of the western North Pacific anomalous anticyclone during the El Niño decaying summer. *Journal of Climate*, *23*(11), 2974–2986. https://doi.org/10.1175/2010JCLI3300.1

Wyrtki, K. (1975). El Niño—The dynamic response of the equatorial Pacific Ocean to atmospheric forcing. *Journal of Physical Oceanography*, *5*(4), 572–584. https://doi.org/10.1175/1520-0485(1975)005<0572:ENTDRO>2.0.CO;2

Yeh, S.-W., Kug, J., Dewitte, B., Kwon, M., Kirtman, B. P., & Jin, F. (2009). El Niño in a changing climate. *Nature*, *461*(7263), 511–514. https://doi.org/10.1038/nature08316

Yu, J.-Y., & Fang, S.-W. (2018). The distinct contributions of the seasonal footprinting and charged-discharged mechanisms to ENSO complexity. *Geophysical Research Letters*, *45*(13), 6611–6618. https://doi.org/10.1029/2018GL077664

Yu, J.-Y., Kao, H.-Y., & Lee, T. (2010). Subtropics-related interannual sea surface temperature variability in the central equatorial Pacific. *Journal of Climate*, *23*(11), 2869–2884. https://doi.org/10.1175/2010JCLI3171.1

Yu, J.-Y., & Kim, S. T. (2011). Relationships between extratropical sea level pressure variations and the Central Pacific and eastern Pacific types of ENSO. *Journal of Climate*, *24*(3), 708–720. https://doi.org/10.1175/2010JCLI3688.1

Yu, J.-Y., Zou, Y., Kim, S. T., & Lee, T. (2012). The changing impact of El Niño on US winter temperatures. *Geophysical Research Letters*, *39*, L15702. https://doi.org/10.1029/2012GL052483

Yuan, Y., & Yang, S. (2012). Impacts of different types of El Niño on the East Asian climate: Focus on ENSO cycles. *Journal of Climate*, *25*(21), 7702–7722. https://doi.org/10.1175/JCLI-D-11-00576.1

Geophysical Research Letters

Supporting Information for

Why does the CP El Niño less frequently evolve into La Niña than the EP El Niño?

Shan He[1,2], Jin-Yi Yu[2], Song Yang[1,3,4], and Shih-Wei Fang[2]

[1]School of Atmospheric Sciences, Sun Yat-sen University, Guangzhou, Guangdong, China, [2]Department of Earth System Science, the University of California at Irvine, Irvine, CA, USA, [3]Guangdong Province Key Laboratory for Climate Change and Natural Disaster Studies, Sun Yat-sen University, Guangzhou, Guangdong, China, [4]Southern Marine Science and Engineering Guangdong Laboratory (Zhuhai), Guangdong, China

Contents of this file

Introduction

This supporting information is comprised of three supplementary texts, eleven supplementary figures, and three supplementary tables.

Text S1.

In Fig. 1b, a late wind reversal (during the decaying February and March) does occur over the western Pacific during the transitional CP El Niño. However, the late reversal is unimportant for the El Niño transition, because the mean thermocline during the spring is deep in the equatorial eastern Pacific. Consequently, SSTs in the eastern Pacific becomes less sensitive to thermocline variation underneath. When the upwelling Kelvin waves induced by the zonal wind reversal in the tropical western Pacific arrive in this region, the thermocline variation cannot effectively change El Niño to La Niña (Y. Jin et al., 2019).

Text S2.

To verify the results from the composite analyses in section 3, we conduct case studies with the transitional Eastern-Pacific (EP) El Niño event in 1972/73, the non-transitional EP event in 1986/87, the transitional Central-Pacific (CP) event in 1987/88, and the non-transitional CP event in 1991/92. We examine wind variations in the tropical western and central Pacific as well as sea surface height (SSH) evolutions during these events (Figs. S7, S8). The results of these case studies support those of the composite analyses (cf. Fig. 1, S3). For the EP El Niño, the reversal of westerly anomalies to easterly anomalies over the western Pacific occurred during the developing November of the 1972/73 transitional event (Figs. S7a, S7c). This wind reversal excited eastward propagation of negative sea surface height (SSH) anomalies (i.e., the upwelling Kelvin waves), which changed the El Niño event into a La Niña event (Figs. S8a–c). During the 1986/87 non-transitional event, however, wind anomalies remained mostly westerlies (Figs. S7b, S7c). Although a wind reversal was seen only in the 1972/1973 transitional event, southward shifts of westerly anomalies over the central Pacific occurred in the developing October of both the 1972/73 transitional and 1986/87 non-transitional events (Figs. S7g–i). Therefore, it is the wind reversal rather than the southward wind shift that can determine whether an EP El Niño event is transitional or non-transitional.

For the CP El Niño, westerly anomalies over the central Pacific shifted southward after the developing November of the 1987/88 transitional event, bringing easterly anomalies into the equatorial Pacific (Figs. S7j, S7l). This southward shift brought about an in-situ change from positive SSH anomalies to negative SSH anomalies along the equatorial central Pacific (Figs. S8d–f), causing the 1987/88 event to evolve into La Niña. In contrast, westerly anomalies remained over the central Pacific during the 1991/92 non-transitional event (Figs. S7k, S7l). For both CP events, a reversal of westerly anomalies to easterly anomalies over the western Pacific did not occur until after the decaying February, long past the period determining their transitions (Figs. S7d–f). Therefore, it is the southward wind shift over the tropical central Pacific rather than the wind reversal over the tropical western Pacific that can determine whether a CP El Niño event is transitional or non-transitional.

Text S3.

To verify the results from the composite analyses in section 4, we again conduct case studies with the transitional EP El Niño event in 1972/73, the non-transitional EP event in 1986/87, the transitional CP event in 1987/88, and the non-transitional CP event in 1991/92. We examine sea level pressure and sea surface temperature anomalies during these events (Figs. S11). The results of these case studies support those of the composite analyses (cf. Fig. 3). For the CP El Niño, the Pacific meridional mode is more distinct in the non-transitional event (i.e., the 1991/92 El Niño; Figs. S11f, S11h) than in the transitional event (i.e., the 1987/88 El Niño; Figs. S11e, S11g). For the EP El Niño, the anomalous Indian Ocean warming and western North Pacific anticyclone are stronger in the transitional event (i.e., the 1972/73 El Niño; Figs. S11a, S11c) than in the non-transitional event (i.e. the 1986/87 El Niño; Figs. S11b, S11d).

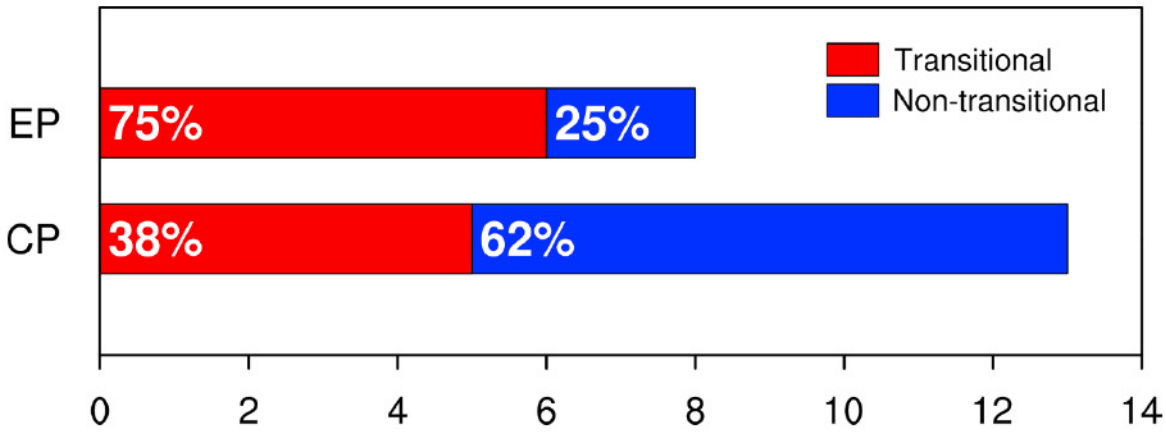

Figure S1. Percentages of the transitional (red) and non-transitional (blue) EP and CP El Niño events.

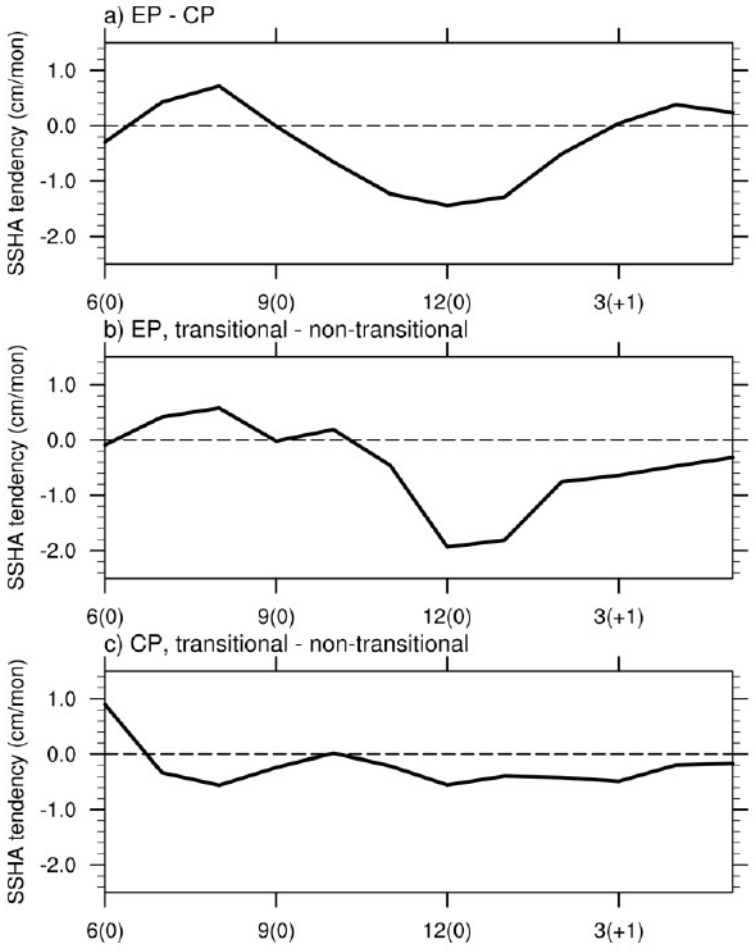

Figure S2. Temporal evolutions of the composite tendencies of SSH anomaly in the equatorial Pacific (5°S–5°N and 155°E–80°W). The evolutions displayed involve (a) the EP El Niño minus the CP El Niño, (b) the transitional group minus the non-transitional group of the EP El Niño, and (c) the transitional group minus the non-transitional group of the CP El Niño, from the developing June to the decaying May.

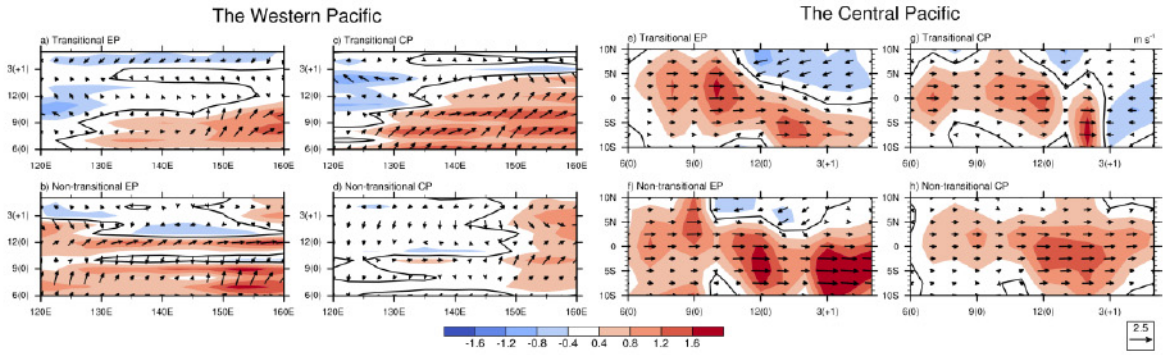

Figure S3. (a, b, c, d) Time-longitude diagrams of the meridional mean composite values of scaled surface wind anomalies (vectors) in the tropical western Pacific and (e, f, g, h) latitude-time diagrams of the zonal mean composite values in the tropical central Pacific from the developing June to the decaying May. Colors denote the zonal components of the composites, and black lines denote the zero contours of the zonal components.

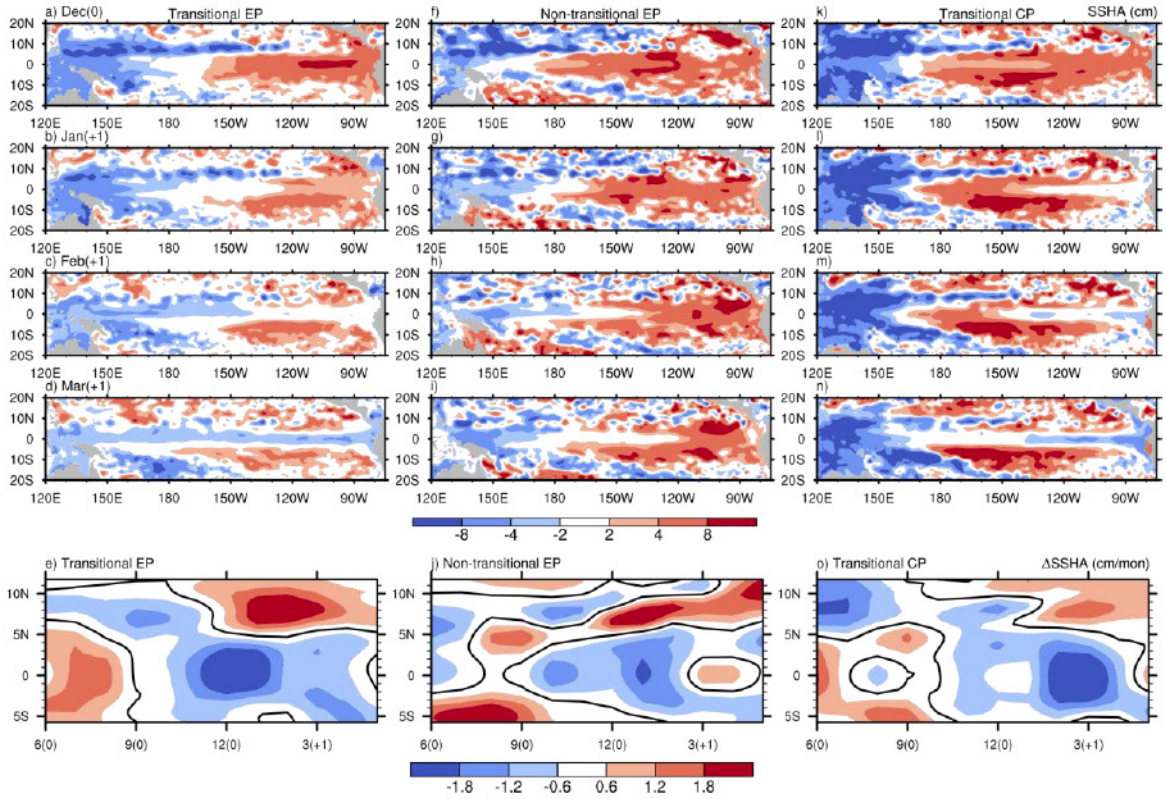

Figure S4. Composite temporal evolutions of scaled SSH anomalies for (a, b, c, d) the transitional EP El Niño, (f, g, h, i) the non-transitional EP El Niño, and (k, l, m, n) the transitional CP El Niño. The Hovmöller diagrams displaying the composite tendencies of scaled SSH anomalies zonally averaged in the tropical central Pacific (160°E–120°W) for (e) the transitional EP El Niño, (j) the non-transitional EP El Niño, and (o) the transitional CP El Niño. (e, j, o) The temporal evolutions displayed are from the developing June to decaying May. Black lines denote zero contours.

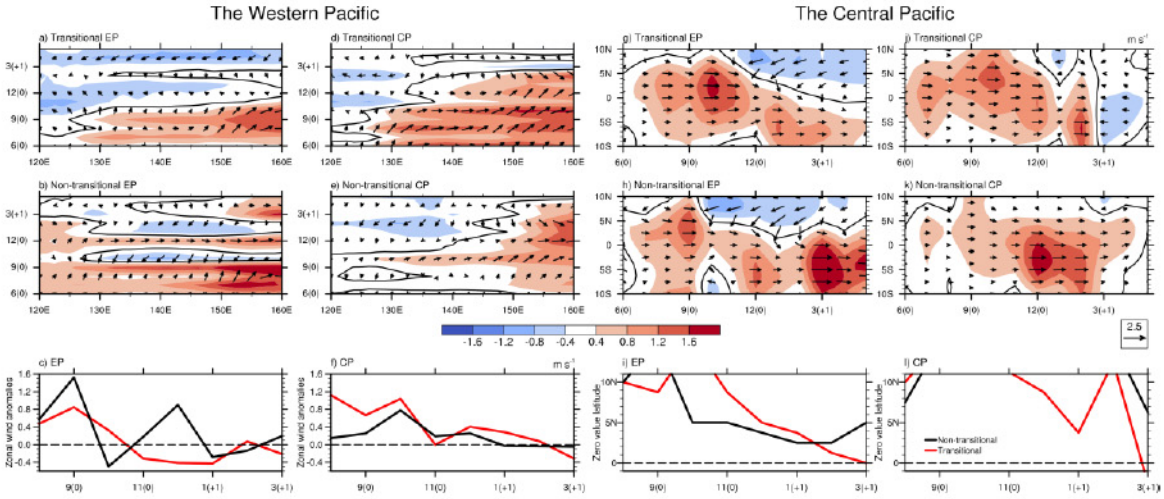

Figure S5. (a, b, d, e, g, h, j, k) As in Fig. S3, except for the anomalies from the JRA-55. (c, f) As in Figs. 1a and, 1b, except for the anomalies from the JRA-55. (i, l) As in Figs. 1d and 1e, except for the latitude of the northern zero contours of the composite scaled zonal wind anomalies from the JRA-55.

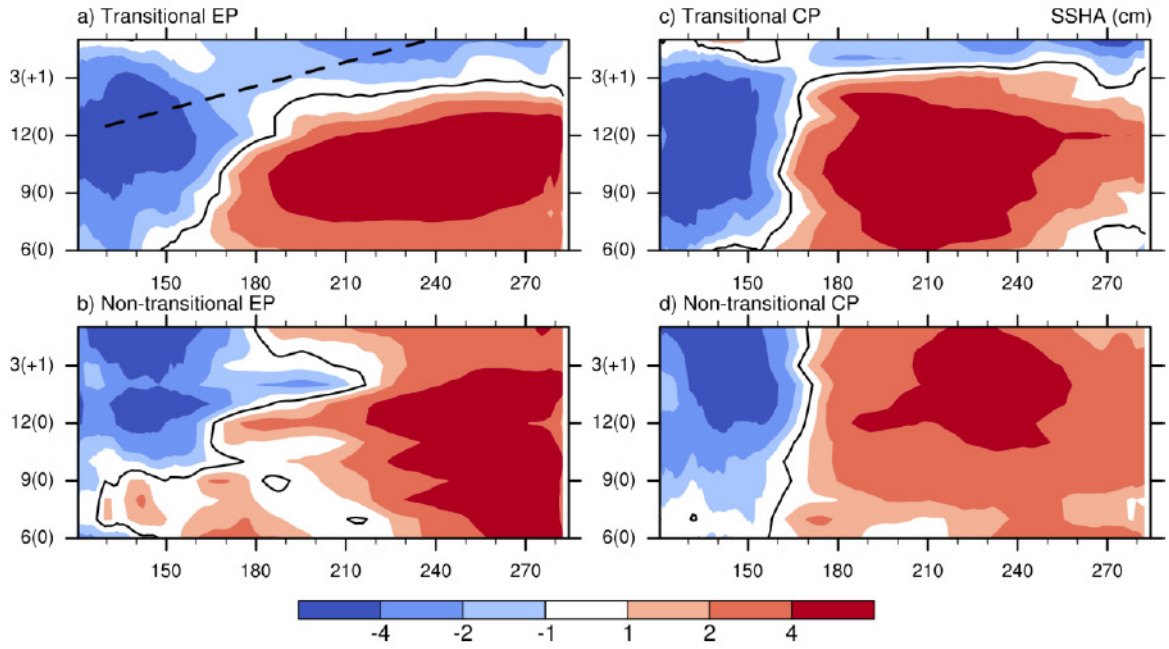

Figure S6. As in Figs. 1g, 1h, 1j, and 1k, except for the anomalies from GECCO3.

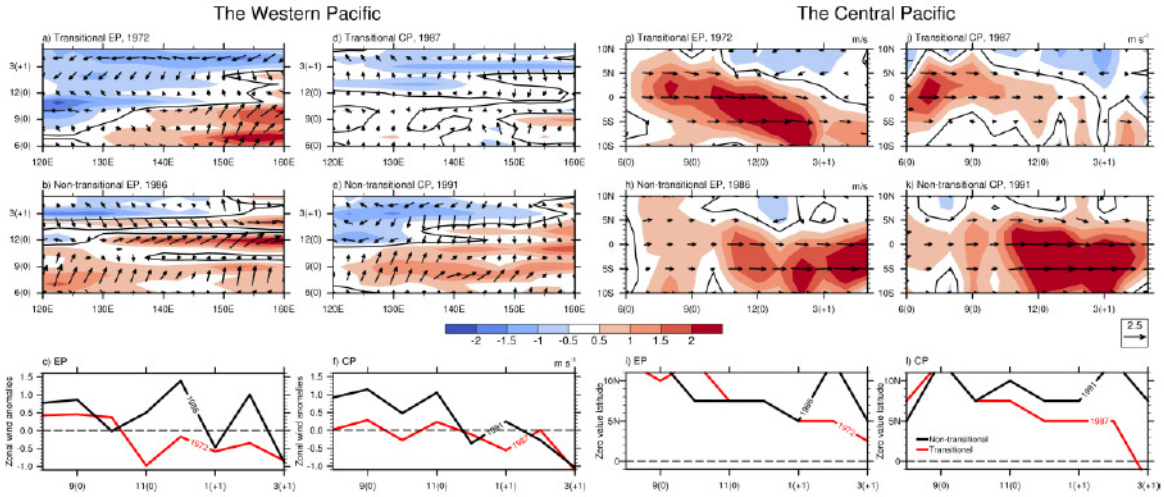

Figure S7. As in Fig. S5, except for the non-scaled values from the NCEP/NCAR Reanalysis of (a, b, c, g, h, i) the transitional EP El Niño event in 1972/73, the non-transitional EP event in 1986/87, (d, e, f, j, k, l) the transitional CP event in 1987/88, and the non-transitional CP event in 1991/92.

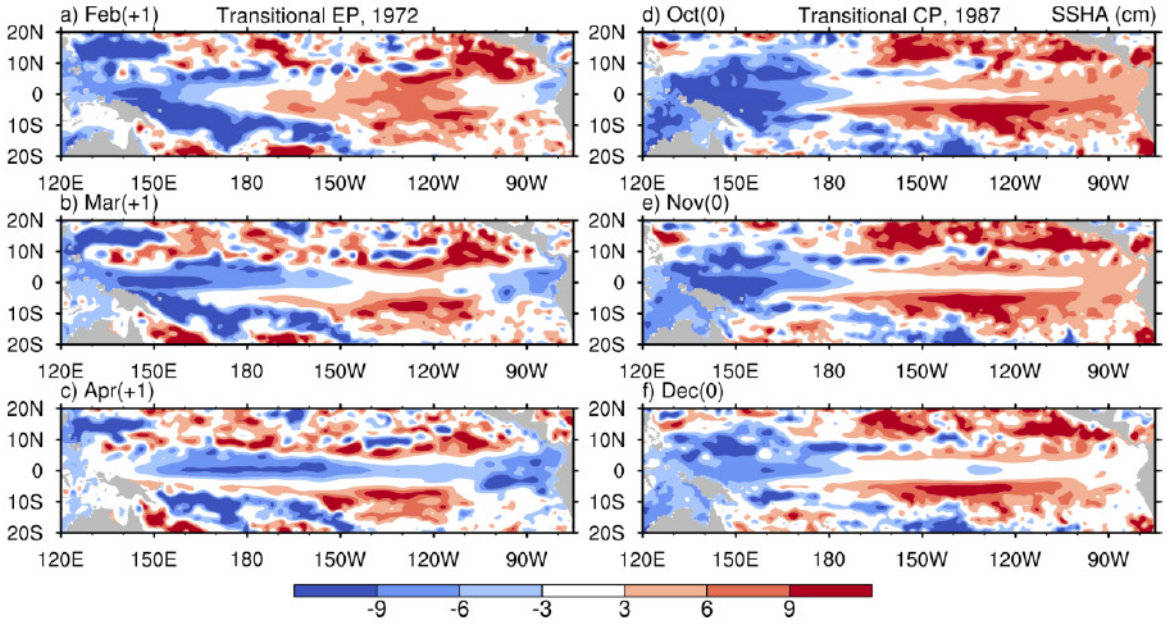

Figure S8. Temporal evolutions of SSH anomalies for (a, b, c) the transitional EP El Niño event in 1972/73 and (d, e, f) the transitional CP event in 1987/88.

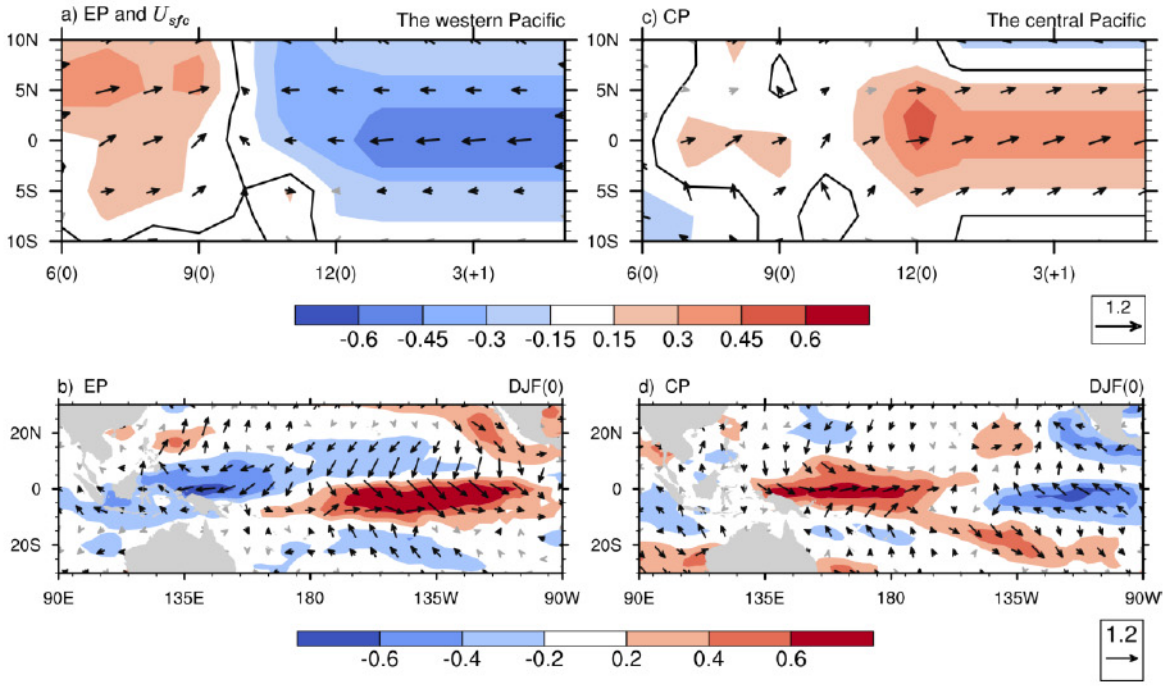

Figure S9. As in Fig. 2, except for the EP and CP indexes defined by Yeh et al. (2009).

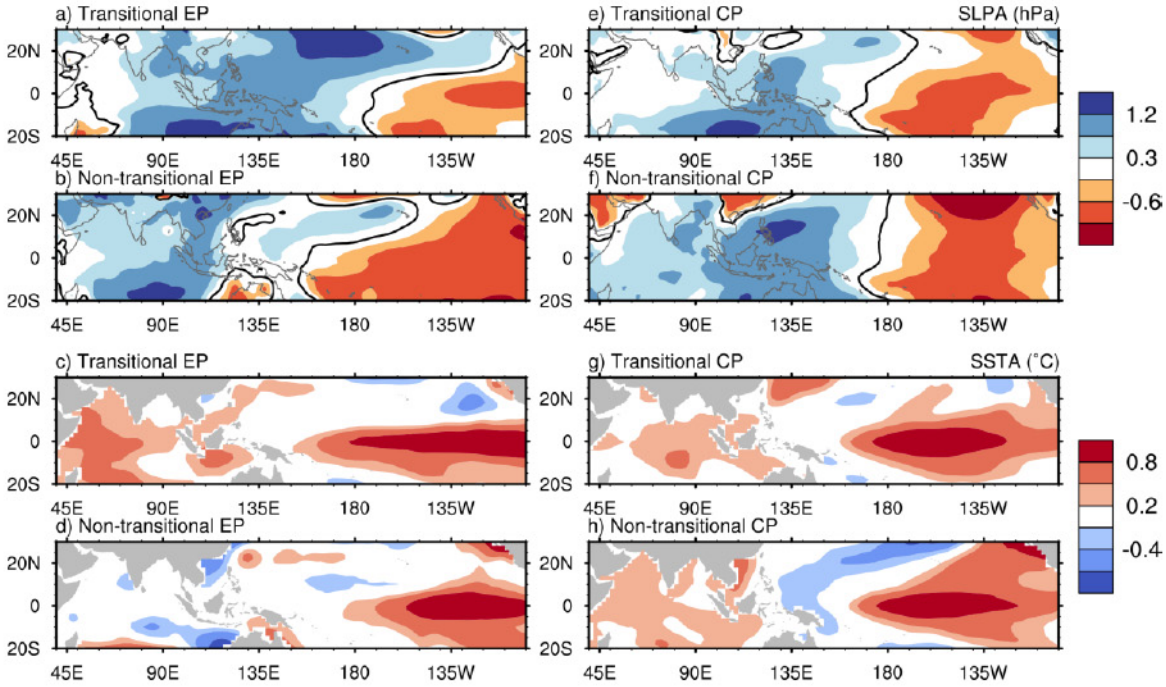

Figure S10. As in Figs. 3a, 3b, 3d, 3e, 3g, 3h, 3j and 3k, except for the anomalies from the JRA-55 and NOAA ERSST V5.

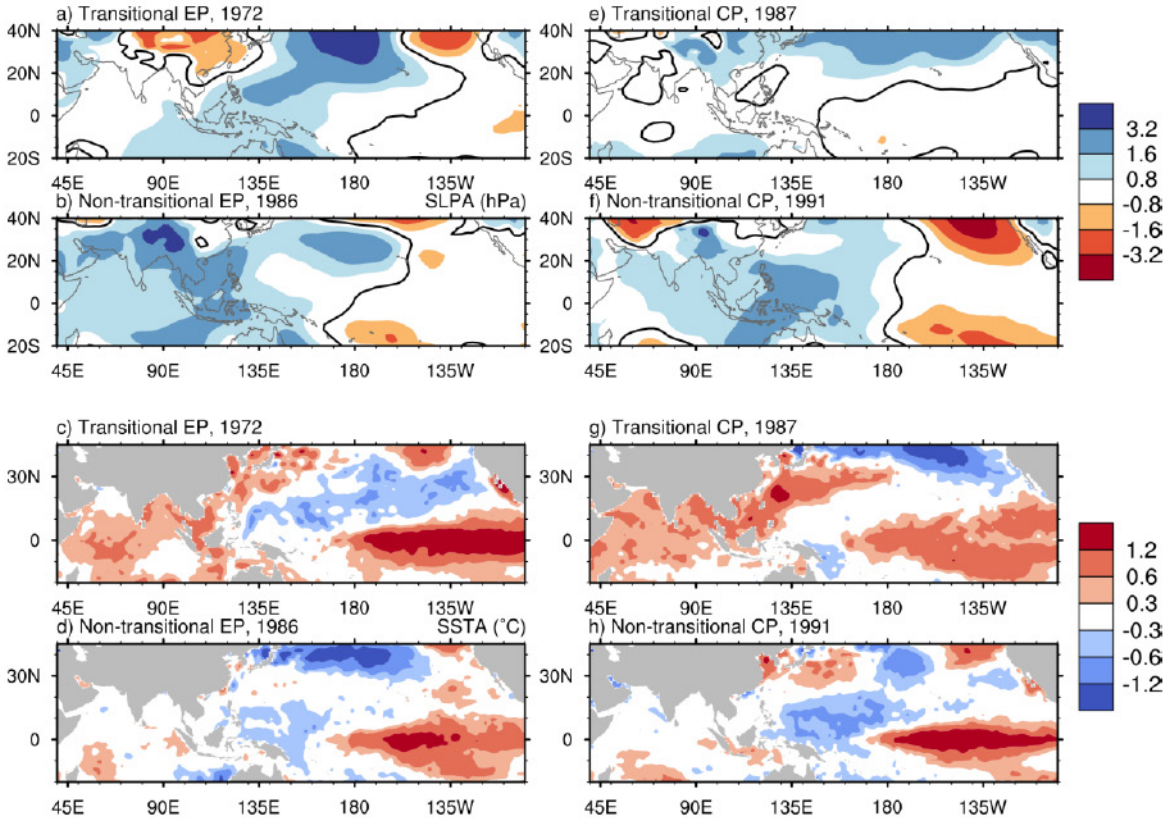

Figure S11. As in Fig. S10, except for the non-scaled values from the NCEP/NCAR Reanalysis of (a, c) the transitional EP El Niño event in 1972/73, (b, d) the non-transitional EP event in 1986/87, (e, g) the transitional CP event in 1987/88, and (f, h) the non-transitional CP event in 1991/92.

	EP El Niño	CP El Niño
Transitional	1969/70, 1972/73, 1982/83, 1997/98, 2006/07, 2015/16	1963/64, 1987/88, 1994/95, 2004/05, 2009/10
Non-transitional	1976/77, 1986/87	1958/59, 1965/66, 1968/69, 1977/78, 1979/80, 1991/92, 2002/03, 2014/15

Table S1. A list of the transitional and non-transitional CP and EP El Niño events.

Year	EP/CP	NIÑO3/4	EMI	Consensus
1958	CP	CP	CP	CP
1963	CP	EP	CP	CP
1965	CP	EP	CP	CP
1968	CP	CP	CP	CP
1969	CP	EP	EP	EP
1972	EP	EP	EP	EP
1976	EP	EP	EP	EP
1977	CP	CP	CP	CP
1979	CP	CP	CP	CP
1982	EP	EP	EP	EP
1986	CP	EP	CP	CP
1987	CP	CP	EP	CP
1991	CP	EP	CP	CP
1994	CP	CP	CP	CP
1997	EP	EP	EP	EP
2002	CP	CP	CP	CP
2004	CP	CP	CP	CP
2006	CP	CP	EP	CP
2009	CP	CP	CP	CP
2014	CP	CP	CP	CP
2015	CP	EP	EP	EP

Table S2. The types of El Niño events identified by the EP/CP index method of Kao and Yu (2009), the NIÑO3/4 index method of Yeh et al. (2009), the El Niño Modoki index (EMI) method of Ashok et al. (2007), and the consensus of these three methods.

La Niña
1964/65, 1970/71, 1971/72, 1974/75, 1975/76, 1983/84, 1984/85, 1988/89, 1995/96, 1998/99, 1999/2000, 2000/01, 2005/06, 2007/08, 2008/09, 2010/11, 2011/12, 2016/17

Table S3. A list of the La Niña events.